ACS OMEGA

http://pubs.acs.org/journal/acsodf

Article

Dual-Labeled Graphene Quantum Dot-Based Förster Resonance Energy Transfer Nanoprobes for Single-Molecule Localization Microscopy

Ju Lu, Shenfei Zong,* Zhuyuan Wang, Chen Chen, Yizhi Zhang, Hong Wang, and Yiping Cui*

Cite This: *ACS Omega* 2021, 6, 8808–8815

Read Online

ACCESS | Metrics & More | Article Recommendations | Supporting Information

ABSTRACT: Single-molecule localization microscopy (SMLM)-based super-resolution imaging techniques (*e.g.*, photoactivated localization microscopy (PALM)/stochastic optical reconstruction microscopy (STORM)) require that the employed optical nanoprobes possess fluorescence intensity fluctuations under certain excitation conditions. Here, we present a dual-labeled graphene quantum dot (GQD)-based Förster resonance energy transfer (FRET) nanoprobe, which is suitable for SMLM imaging. The nanoprobe is constructed by attaching Alexa Fluor 488 (AF488) and Alexa Fluor 568 (AF568) dye molecules onto GQDs. Experimental results confirmed the FRET effect of the nanoprobes. Moreover, under a single 405 nm excitation, the FRET nanoprobe exhibits excellent blinking behavior. SMLM imaging of microtubules in MRC-5 cells is realized. The presented nanoprobe shows great potential in multicolor SMLM-based super-resolution imaging.

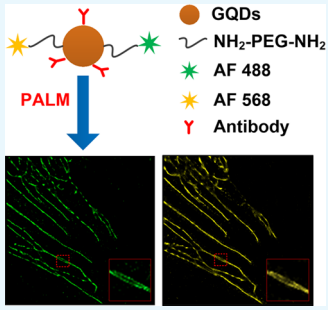

INTRODUCTION

Optical microscopy is one of the key methods in current medical science and life science research. Among the various microscopy techniques, fluorescence microscopy is the essential tool to study structures and dynamics in cells and tissues. However, conventional fluorescence microscopy is limited by relatively low spatial resolution because of the diffraction limit of light. In recent years, super-resolution imaging techniques that break the diffraction limit have become a promising tool to allow optical imaging of many biological structures with up to molecular-scale resolution.[1−3]

Super-resolution imaging techniques can be classified into the following two categories based on the mechanism of surpassing the diffraction limit: (i) illumination pattern-based approaches, such as stimulated emission depletion microscopy (STED)[4,5] and structured illumination microscopy (SIM);[6] (ii) single-molecule localization microscopy (SMLM),[7] including (fluorescence) photoactivated localization microscopy (PALM/fPALM),[8,9] (direct) stochastic optical reconstruction microscopy (STORM/dSTORM),[10−12] etc.

Among various super-resolution imaging techniques, single-molecule localization microscopy (SMLM) including PALM and STORM can provide the highest spatial resolution.[13] The common nanoprobes used in SMLM include fluorescent protein (*e.g.*, green fluorescent protein),[14−16] fluorescent dyes (*e.g.*, Alexa Fluor 647),[17,18] and quantum dots (QDs).[19,20] SMLM requires stochastic blinking of specific fluorescent nanoprobes, and this blinking behavior permits them to be observed one at a time so that their spatial coordinates can be localized with subdiffraction precision.[21,22] Usually, blinking behavior is an intrinsic property of fluorescent proteins (PALM) or specific organic dyes (STORM), which can be provoked by specific excitation conditions (multi lasers to activate and excite the nanoprobes) and buffer conditions (imaging buffer containing a primary thiol and an oxygen-scavenging buffer), which limit the application in long-term live cell imaging.[17,18,22]

Förster resonance energy transfer (FRET) is a non-radiative process in which an excited dye donor transfers energy to an acceptor dye in the ground state through long-range dipole−dipole interactions. FRET-based nanoprobes have been widely used to study replication, recombination, transcription, translation, RNA folding, and catalysis.[23−26] Herein, we present a graphene quantum dot (GQD)-based dual-labeled FRET nanoprobe with excellent fluorescence intensity blinking behavior suitable for SMLM. The structure of the FRET nanoprobes is illustrated in Scheme 1. In general, the FRET nanoprobe is constructed by attaching AF488 and AF568 dye molecules onto the surfaces of GQDs. GQDs serve as the donor and the AF488 and AF568 dye molecules as the acceptor. GQDs are chosen as the donor because of their fine solubility, stable fluorescence, excellent biocompatibility, and minimal toxicity.[27−29] In our previous work, we have described a GQD-based nuclear-targeted drug delivery system, which enables real-time monitoring of the release process through FRET.[30] Alexa Fluor dyes are common fluorescent dyes widely used in SMLM and

Received: November 6, 2020
Accepted: March 5, 2021
Published: March 24, 2021

Scheme 1. Schematic Illustration of the FRET Nanoprobes

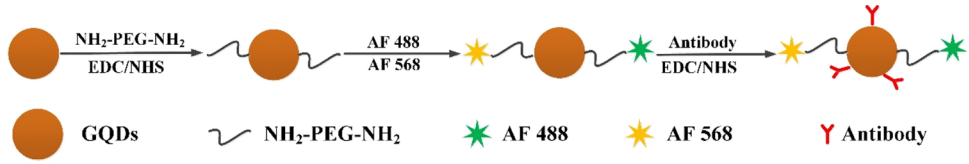

thus are chosen as the acceptor in our experiment. Experimental results confirmed that the FRET effect is observed under a single 405 nm laser excitation of the dual-labeled nanoprobes. In addition, dual-labeled SMLM imaging of the microtubule in MRC-5 cells is realized using the FRET nanoprobe.

RESULTS AND DISCUSSION

Characterization of the FRET Nanoprobes. The structure of the FRET nanoprobes is illustrated in Scheme 1. First, GQDs were modified with PEG-NH_2 via EDC/NHS cross-linking reaction. The PEG component offered a greatly enhanced biocompatibility, while the remaining amino group attached to PEG was further used to conjugate the carboxyl group of Alexa Fluor NHS ester.[31] Then, antibodies were labeled via standard carboxyl-amine conjugation chemistry. Thus, the FRET nanoprobes were formed.

The transmission electron microscopy (TEM) images are used to characterize the morphology of the FRET nanoprobes, and the results are shown in Figure 1a,b. Figure 1a and Figure 1b

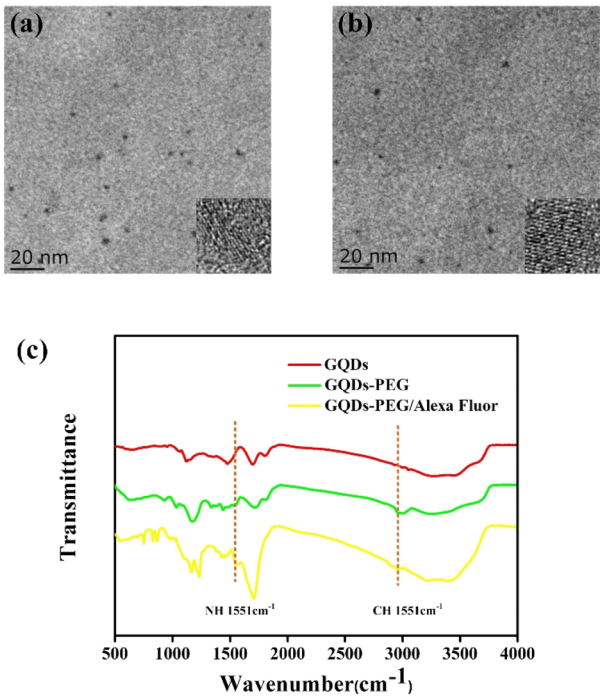

Figure 1. TEM and FTIR characterization: (a) TEM images of GQDs; (b) TEM images of the FRET nanoprobes; (c) FTIR spectra of GQDs, GQDs-PEG, and the dual-labeled FRET nanoprobes.

show the TEM images of GQDs and the FRET nanoprobes, respectively. The high-resolution TEM (HR-TEM) images are shown in the inset. As can be seen, the well-dispersed GQDs have an average diameter of about 5 nm. The lattice of GQDs is regular with a *d*-spacing of 0.212 nm corresponding to the facet of graphene. As the organic dye is invisible in TEM images, the FRET nanoprobes have a similar morphology compared to GQDs. The results confirmed that the fabrication procedure does not significantly change the character of GQDs.

The optical characterization of the FRET nanoprobe is subsequently performed, and the results are shown in Figure 2. Figure 2a shows the fluorescence spectrum of GQDs. When being excited at 405 nm, the fluorescence emission peak was located at 512 nm, displaying a green photoluminescence (PL). As can be seen, the emission spectrum of GQDs is relatively wide. Here, AF488 and AF568 were chosen as the candidate dye molecules to confirm that the FRET nanoprobes can be used to excite different fluorescence signals under 405 nm illumination. Figure 2b shows the normalized PL spectra of the FRET nanoprobe with AF488, AF568, and AF488&568. As can be seen, distinctive emission peaks around 525 and 600 nm can be observed attributed to the emission of AF488 and AF568. This confirmed the FRET effect of the nanoprobes with different organic dyes.

In addition, the functionalization procedures were characterized in detail by Fourier transform infrared (FTIR) spectroscopy, and the results of the FRET nanoprobe are shown in Figure 1c. Compared with the spectrum of GQDs, two new peaks at 2957 (asymmetric stretching of C−H) and 1551 cm^{-1} (asymmetric stretching of N−H) assigned to the attached NH_2-PEG-NH_2 can be observed from the spectrum of GQDs-PEG. Peaks at 3430 (stretching vibration of O−H) and 1365 cm^{-1} (bending vibration of O−H) are also presented. In addition, peaks at 3150 cm^{-1} (stretching of amide N−H) proved the successful conjugation of NH_2-PEG-NH_2. After Alexa Fluor dyes were attached, peaks at 1704 and 1551 cm^{-1} ascribed to the carbonyl stretching of −COOH and the asymmetric stretching of N−H were found, and peaks at 1650 cm^{-1} (stretching of amide C═O) confirmed the successful conjugation of Alexa Fluor dyes.

The luminescence quantum yield (QY) is measured using the following equation and Rhodamine B solution as the reference sample, whose QY is 31% under 514 nm excitation.[32]

$$Q = Q_R \frac{I}{I_R} \frac{\mathrm{OD}_R}{\mathrm{OD}} \frac{n^2}{n_R^2}$$

In the equation, Q is the quantum yield, I is the integrated intensity, n is the refractive index, and OD is the optical density. The subscript R refers to the reference fluorophore of a known quantum yield. By calculation, the QY values of GQDs and the FRET nanoprobes are 28.3 and 3.4%, respectively. According to the experimental results, the QY of the nanoprobes is lower than GQDs due to the introduction of nonradiative carrier traps in the modification and antibody labeling procedure. However, considering the high sensitivity of the Andor EM-CCD camera (iXonDU897) used in our experiments, the nanoprobes with such a QY are still applicable for SMLM imaging. Fluorescence lifetime (FL) is also characterized to confirm the FRET effect. Fluorescence lifetime of a photophysical process is the time required by a population of N electronically excited molecules to

https://doi.org/10.1021/acsomega.0c05417
ACS Omega 2021, 6, 8808−8815

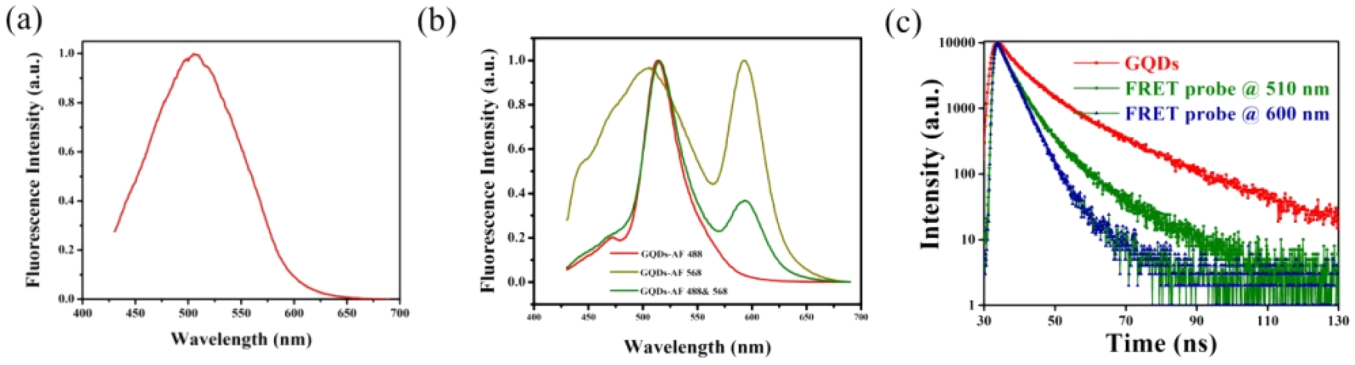

Figure 2. PL spectra and fluorescence lifetime characterization: (a) PL spectra of GQDs; (b) PL spectra of the FRET nanoprobes; (c) fluorescence lifetime measurement of GQDs and the FRET nanoprobes.

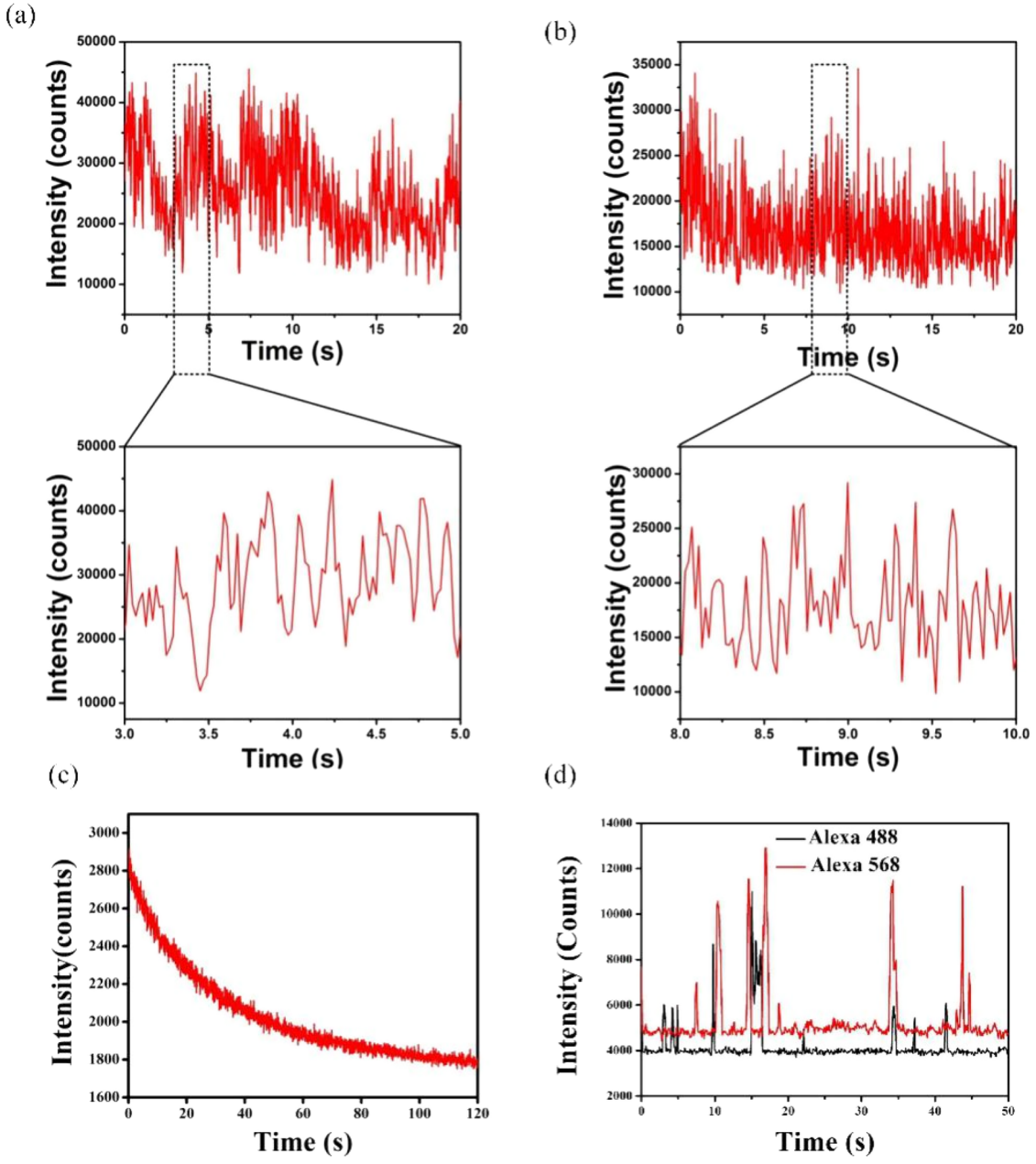

Figure 3. Single-particle analysis of the (a) FRET nanoprobe labeled with only AF488; (b) FRET nanoprobe labeled with only AF568; (c) GQDs; (d) FRET nanoprobe labeled with both AF488 and AF568.

https://doi.org/10.1021/acsomega.0c05417
ACS Omega 2021, 6, 8808−8815

be reduced by a factor of e. The FL values of GQDs and AF488 and AF568 channels of the dual-labeled FRET nanoprobes are shown in Figure 2c. The FL at 510 nm corresponds to the AF488 channel, while the FL at 600 nm corresponds to the AF568 channel. GQDs are excited under 405 nm, and FL at 512 nm is measured. The FRET nanoprobes are excited under 405 nm, and the FL values at 510 and 600 nm are measured. The obtained time-dependent fluorescence decay profile is fitted using the equation

$$I(t) = A + B_1 \exp(-t/\tau_1) + B_2 \exp(-t/\tau_2) + B_3 \exp(-t/\tau_3)$$

The FL values of GQDs and the AF488 and AF568 channel of the FRET nanoprobes are determined to be 6.25, 3.37, and 3.46 ns, respectively. The FL values of AF488 and AF568 are determined to be 4.1 and 3.6 ns, respectively (data from the manufacturer). PL lifetime delays were measured using a PluoroLog 3-TCSPC spectrometer, and the PL lifetime was obtained by fitting the PL decay spectra with a double-exponential equation. GQDs show an FL of 6.25 ns, which reduced to 3.37 and 3.46 ns in the two channels of the FRET nanoprobes. The FL of the acceptor channels is close to those of AF488 and AF568, indicating that the FL of FRET nanoprobes is mainly influenced by the acceptor. The fabrication procedure of the FRET nanoprobes will cause reduction in the QY due to the introduction of more nonradiative carrier traps.[33,34] To further investigate the difference in fluorescence lifetime, an experiment was done to confirm whether FRET occurs solely from the GQDs to the two fluorophores. The fluorescence spectrum of the dual-labeled nanoprobes under 488 nm laser excitation is shown in Figure S2. As shown in Figure S2, under 488 nm excitation, an emission peak around 600 nm can be observed attributed to the emission of Alexa Fluor 568. In addition, the fluorescence lifetime of the dual-labeled nanoprobe (Alexa Fluor 488 channel) under 488 nm excitation was determined to be 3.83 ns. Both experimental results confirm the existence of cascade-type FRET.

Single-Molecule Analysis of the FRET Nanoprobe. The above experimental results have confirmed the FRET effect of the nanoprobes. However, a prerequisite for nanoprobes used in SMLM imaging is that their fluorescence intensity must process blinking or fluctuation under certain excitation conditions. The single-molecule analysis of the FRET nanoprobes is subsequently investigated using a Zeiss Elyra P.1 system. The experiment was performed in phosphate buffered saline (PBS). Figure 3a and Figure 3b show typical time-dependent fluorescence intensity profiles of an individual single-labeled FRET nanoprobe at the AF488 channel and AF568 channel, respectively. As contrast, single-molecule analysis of the dual-labeled FRET nanoprobes with AF488 and AF568 is also investigated and the results are shown in Figure 3d. The exposure time is 20 ms, and the filters were set as BP 495-575 for the AF488 channel and BP 570-650 for the AF568 channel. The enlarged images are shown in the panel below. Two properties of switchable probes crucial to the super-resolution image quality are (i) the number of photons detected per switching event and (ii) the on−off duty cycle (or the fraction of time a fluorophore spends in the on state).[21] Experimental results confirm that, under continuous 405 nm laser excitation, the dual-labeled FRET nanoprobes blink markedly with the change of time. Furthermore, compared to the single-labeled FRET nanoprobe, dual-labeled FRET nanoprobes exhibit a lower on−off duty cycle and the blinking behavior is better. As is well known, stochastic blinking of fluorescence intensity is a prerequisite of SMLM imaging. Consequently, the excellent blinking effect of the proposed dual-labeled FRET nanoprobes indicates potential for SMLM application.

Moreover, the single-particle analysis of GQDs immersed in PBS solution is also studied and the result is shown in Figure 3c. It can be observed that, under continuous 405 nm laser excitation, the fluorescence intensity gradually decays over time and without obvious blinking behavior. This confirmed that the blinking behavior of the FRET nanoprobe is caused by the FRET effect of the nanoprobes.

Switching properties of the presented dual-labeled nanoprobe are given in Table 1, and compared to the switching properties of common organic dyes, the presented nanoprobe exhibits great switching properties similar to organic dyes. In addition, according to the Lambert−Beer law, the molar concentration of GQDs can be measured by UV−vis spectrum characterization, and we can use the extinction spectra to determine the concentration of dye molecules in the FRET nanoprobes by comparing the absorbance value with dye standard solutions; the per number of dye molecules that bond to GQDs can be roughly calculated (~6.8).

Table 1. Switching Properties of the Presented Nanoprobes

	detected photos per switching events	on−off duty cycle	number of switching cycles
Alexa Fluor 488 channel	8200	0.00095	82
Alexa Fluor 568 channel	6100	0.00086	35

SMLM Imaging with the FRET Nanoprobes. In our previous experiment, the dual-labeled FRET nanoprobes have been shown to process the fluorescence blinking property and are suitable for SMLM imaging. Before SMLM imaging, the MTT assay was performed to investigate the cytotoxicity of the FRET nanoprobe with different GQD concentrations, and the FRET nanoprobe shows quite low cytotoxicity, as shown in Figure S1; different doses of GQDs (25−200 μg/mL) do not weaken the cell activity.

Then, the FRET nanoprobes were applied to cell imaging. Immunofluorescence imaging of microtubules using the FRET nanoprobe was performed in MRC-5 cells. MRC-5 cells were immunostained with primary antibodies and then labeled with the FRET nanoprobes. The fluorescence signals were collected with different filters under 405 nm laser excitation. The filters were set as BP 495-575 for the AF488 channel and BP 570-650 for the AF568 channel. The SMLM images of the AF568 channel were reconstructed followed by the AF488 channel. The fluorescence image and SMLM images are shown in Figure 4. The SMLM images show a drastic improvement in the resolution of the microtubule network as compared to the conventional fluorescence image. In the regions where microtubules were densely packed and undefined in the conventional fluorescence image, individual microtubule filaments were clearly resolved in SMLM images at both channels (red box in Figure 4a−c). To determine the imaging resolution more quantitatively, we measured the apparent width of an individual microtubule filament in the SMLM images by examining the cross-sectional profile. Cross-sectional distribution of localization (Figure 4g) for a microtubule segment, as indicated by the red line in Figure 4b,c, is measured. The Gaussian fit to the

https://doi.org/10.1021/acsomega.0c05417
ACS Omega 2021, 6, 8808−8815

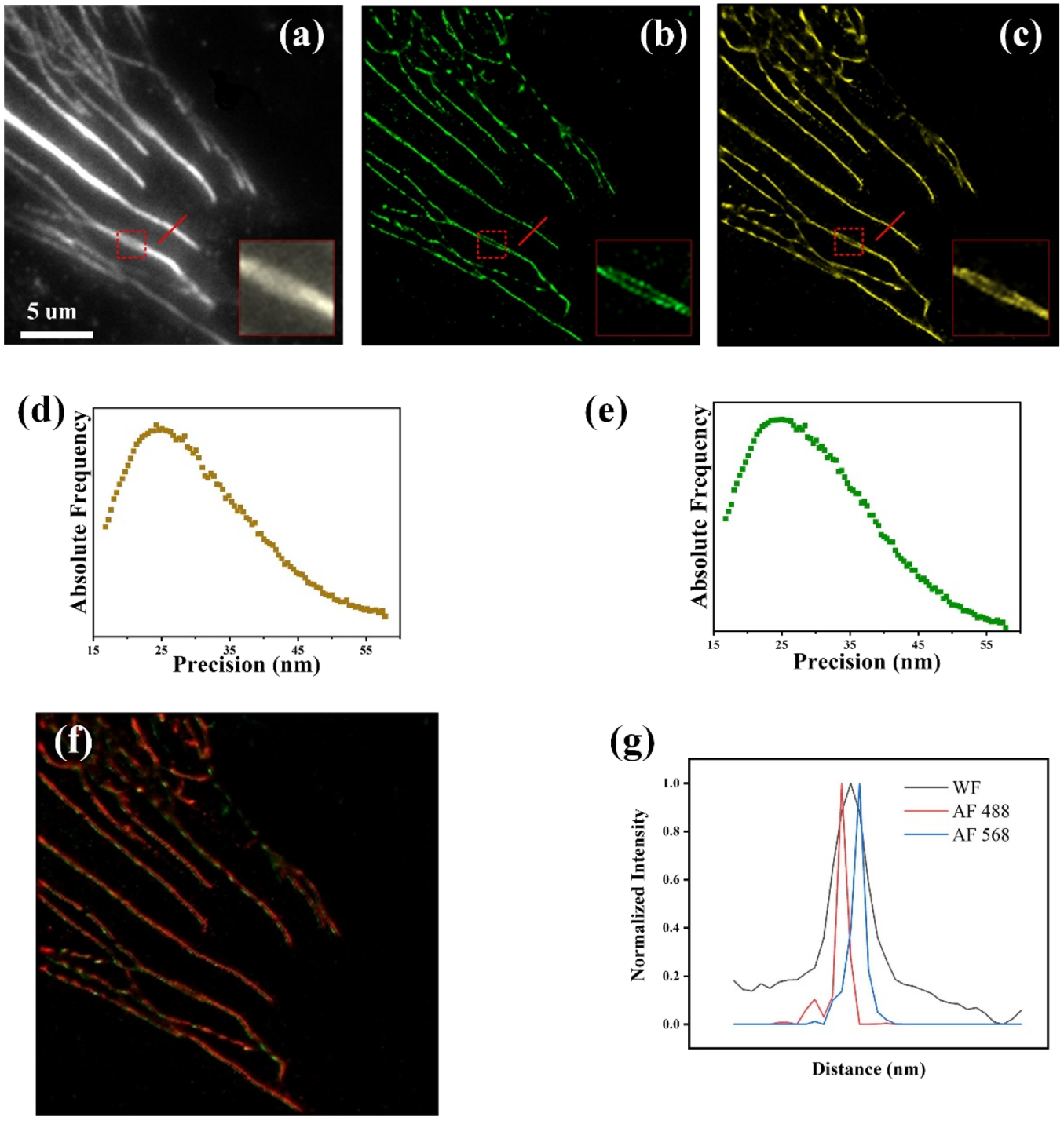

Figure 4. SMLM imaging of the microtubules in MRC-5 cells. (a) Conventional widefield image of the microtubules in MRC-5 cells; (b, c) SMLM images of the same area with the FRET nanoprobes at the AF488 channel (b) and AF568 channel (c); (d, e) localization precision of panels (b, c); (f) merged image of panels (b, c); (g) cross-sectional profiles of the region, as indicated by the red lines in panels (a−c).

profile yielded a full width at half-maximum (FWHM) of ∼50 nm in both channels (Figure 4b,c). The localization precision of SMLM imaging is ∼25 nm at both channels, as acquired by the analyzing software of the Elyra P.1 system, which is obviously higher than conventional fluorescence microscopy. More importantly, as shown in the merged image (Figure 4f), the microtubule filament is more continuous and more details are shown.

DISCUSSION AND CONCLUSIONS

A different route to SMLM is PAINT (point accumulation for imaging in nanoscale topography); freely diffusing dyes or dye-labeled ligands target molecules by permanent or transient binding. Specifically, DNA-PAINT has been developed to overcome some limitations of super-resolution techniques. In DNA-PAINT, repeated imaging, washing, and reintroduction of new imager strand species are exploited to achieve necessary blinking. However, the nonfluorogenic nature of imager strands

https://doi.org/10.1021/acsomega.0c05417
ACS Omega 2021, 6, 8808−8815

is limited to the achievable image acquisition speed as compared with SMLM. Furthermore, DNA-PAINT applications are currently limited to fixed specimens. Live cell imaging could be more difficult to achieve as compared with the other SMLM techniques.

Compared with DNA-PAINT, fluorescence blinking of the dual-labeled FRET nanoprobe is caused by the FRET effect, and SMLM imaging of the dual-labeled FRET nanoprobe does not require a specific thiol containing buffer; consequently, the nanoprobe is suitable for live cell SMLM imaging. The advantages of the dual-labeled FRET nanoprobe mainly include single-laser excitation, non-special imaging buffer, low cytotoxicity, and excellent blinking behavior; these properties can simplify imaging conditions and are quite suitable for live cell imaging.

In conclusion, the FRET nanoprobe was successfully fabricated using GQDs as the donor and the AF488 and AF568 channel as the acceptor. The FRET nanoprobe can be excited under a single 405 nm laser excitation. Time-dependent single-particle analysis confirmed that the FRET nanoprobes exhibit fluorescence blinking behavior. SMLM imaging of microtubules in MRC-5 cells was realized using the proposed FRET nanoprobe with a localization precision of ∼25 nm. The advantages of the dual-labeled FRET nanoprobe mainly include single-laser excitation, non-special imaging buffer, low cytotoxicity, and excellent blinking behavior, and these properties can simplify imaging conditions and are quite suitable for live cell imaging. Compared with common organic dyes used in SMLM, the presented nanoprobe exhibits similar switching properties, and in SMLM imaging, a single laser was used and does not need special imaging buffer. However, considering the occupation of multiple channels, the application in multicolor imaging is limited. Even so, the presented dual-labeled FRET nanoprobe can also be applied to imaging different organelles, enhancing our ability to visualize molecular interactions in cells and tissues.

EXPERIMENTAL SECTION

Materials. Graphite powder was purchased from Sinopharm Chemical Reagent Co., Ltd. Dimethylformamide (DMF), 1-ethyl-3-(3-dimethylaminopropyl)carbodiimide (EDC), and *N*-hydroxysuccinimide (NHS) were purchased from Sigma-Aldrich. NH_2-PEG-NH_2 (M_w = 2000) was purchased from Jenkem Co., Ltd. Poly(ethylene imine) (PEI, M_w = 15,000) was purchased from Alfa Aesar. Alexa Fluor NHS ester and Goat anti mouse IgG were purchased from Thermo Fisher Scientific. Phosphate buffered saline (PBS, pH 7.4) was purchased from Beijing Biosynthesis Biotechnology Co., Ltd. All the reagents were used as received. Deionized water (Millipore Milli-Q grade) with a resistivity of 18.2 MΩ/cm was used in all the experiments.

Preparation of Graphene Quantum Dots (GQDs). Graphene oxide (GO) was prepared by the modified Hummers method using graphite powder as the starting meterial.[35] Typically, 1 g of graphite powder was stirred in 23 mL of H_2SO_4 (98%) overnight. Afterward, 4 g of $KMnO_4$ was gradually added, the mixture was stirred for 60 min in an ice bath, and then stirred at 40 °C for 30 min. Next, the temperature was increased to 100 °C, and the mixture was diluted to 100 mL with water and stirred for another 30 min. Subsequently, 10 mL of H_2O_2 (30%) solution was added and the color of the mixture changed to bright yellow quickly. The mixture was washed by repeated centrifugation and filtration, first with HCl aqueous solution (5%) and then distilled water until the pH of the solution became neutral. To exfoliate the oxidized graphite, the product was treated with an ultrasonic probe at 400 W for 30 min and GO was obtained followed by centrifugation.

The GQDs were prepared through a facile one-pot solvothermal method.[36] In brief, GO was dissolved in dimethylformamide (DMF) at a concentration of ∼200 mg/mL. The mixture was first ultrasonicated for 40 min (120 W, 100 kHz), then transferred to a poly(tetrafluoroethylen)-lined autoclave (100 mL), and heated at 200 °C for 6 h. After cooling to room temperature, the obtained mixture was filtered through a 0.22 μm microporous membrane to remove the precipitates, obtaining a brown solution. Excess DMF was removed by evaporation. Finally, the obtained GQD was further dialyzed using a dialyzer (500 Da) to remove the DMF residues completely.

PEGylation of GQDs. In brief, 12 mg of EDC and 18 mg of NHS were added to 5 mL of the as-prepared GQD solution. The mixture was ultrasonicated for 1 min and stirred for 30 min at room temperature. Then, 1 mL of NH_2-PEG-NH_2 solution (50 mg/mL in PBS) was added to the mixture and reacted for 6 h. The solution was dialyzed using a dialyzer (3500 Da) and further purified by ultrafiltration (Amicon Ultra-15, 3 KD, Millipore).

Preparation of the FRET Nanoprobes. Alexa Fluor NHS ester was covalently conjugated onto amine-functionalized GQDs-PEG through the carboxyl group (−COOH). In a typical experiment, 1 μL of 0.1 mM of Alexa Fluor NHS ester was added to as-prepared GQD-PEG solution. The mixture was shaken for 4 h at room temperature. Excess Alexa Fluor dyes were removed by dialysis (3500 Da). The obtained solution was concentrated by ultrafiltration (Amicon Ultra-15, 3 KD, Millipore) and redispersed in PBS solution.

Antibody Labeling of the FRET Nanoprobes. The antibody labeling of the FRET nanoprobes was according to the following procedure. Goat anti-mouse IgG (100 μL) was added to 2 mL of the GQD-Alexa Fluor dye solution pretreated with EDC and NHS. The mixture was shaken for 4 h at room temperature and further reacted at 4 °C overnight, and the obtained solution was concentrated by ultrafiltration (Amicon Ultra-15, 50 KD, Millipore).

Cell Immunostaining. Human embryonic lung fibroblast (MRC-5) cells were purchased from China Type Culture Collection. Cells were kept under standard cell culture conditions (5% CO_2, 37 °C). The culture media (Dulbecco's modified Eagle's medium, DMEM) were supplemented with 10% fetal bovine serum (GIBCO) and 1% penicillin−streptomycin (Nanjing KeyGen Biotech. Co., Ltd.). For fluorescence imaging, MRC-5 cells were seeded into cell culture dishes and incubated for 24 h before use. Microtubules were immunostained using the following procedure: washing in PBS; fixation in a mixture of 4% paraformaldehyde and 0.1% glutaraldehyde in PBS for 20 min; 3× washing with PBS; reduction with 1 mg/mL of $NaBH_4$ for 7 min; 3× washing with PBS; permeabilization with 0.2% (v/v) Triton X-100 in PBS for 30 min; 3× washing with PBS; blocking with 3% (w/v) bovine serum albumin (BSA) for 90 min and staining overnight with the mouse antibody against β-tubulin; 3× washing with PBS; post-fixation in a mixture of 4% paraformaldehyde and 0.1% glutaraldehyde in PBS for 10 min.

Single-Molecule Analysis. The FRET nanoprobes and GQDs were immobilized onto the bottom of cell culture dishes as follows. First, the bottom of the cell culture dish was modified with PEI (0.1%) for 20 min to introduce amino groups. Then, excess PEI was washed away with water. FRET nanoprobes (4

https://doi.org/10.1021/acsomega.0c05417
ACS Omega 2021, 6, 8808−8815

μL) were added into 120 μL of deionized water. After ultrasonication for 10 s, the diluted FRET nanoprobes were added into the cell culture dishes and incubated for 20 min to allow electrostatic adsorption of the nanoprobes. After washing away excess FRET nanoprobes with water, 120 μL of imaging buffer was added into the cell culture dish, which was subsequently imaged using a Zeiss Elyra P.1 microscope. The immobilization of GQDs followed the same method, as described above.

Instruments. Extinction spectra were recorded by using a Shimadzu UV-3600 PC spectrophotometer with quartz cuvettes of a 1 cm path length. Photoluminescence emission spectra were recorded by using an Edinburg FLS 920 spectrofluorometer. Transmission electron microscopy (TEM) images were obtained with an FEI Tecnai G2T20 electron microscope operating at 200 kV. Fluorescence and SMLM images were acquired using a Zeiss Elyra P.1 microscope equipped with 405 (50 mW), 488 (100 mW), 561 (100 mW), and 640 nm (150 mW) lasers. Fluorescence images were recorded using a 100×/1.46 oil immersion objective and an Andor EM-CCD camera (iXon DU897). Imaging data were analyzed using the Zeiss Zen 2012 software.

■ ASSOCIATED CONTENT

Supporting Information

The Supporting Information is available free of charge at https://pubs.acs.org/doi/10.1021/acsomega.0c05417.

> Cell viability after incubation with the FRET nanoprobe, fluorescence spectrum of the dual-labeled nanoprobe under 488 nm excitation, and SMLM images of the live MRC-5 cell incorporated with the FRET nanoprobe (PDF)

■ AUTHOR INFORMATION

Corresponding Authors

Shenfei Zong − *Advanced Photonics Center, Southeast University, Nanjing 210096, Jiangsu, China*; Email: sfzong@seu.edu.cn

Yiping Cui − *Advanced Photonics Center, Southeast University, Nanjing 210096, Jiangsu, China*; orcid.org/0000-0002-4648-2506; Email: cyp@seu.edu.cn

Authors

Ju Lu − *Advanced Photonics Center, Southeast University, Nanjing 210096, Jiangsu, China*

Zhuyuan Wang − *Advanced Photonics Center, Southeast University, Nanjing 210096, Jiangsu, China*; orcid.org/0000-0003-1262-5342

Chen Chen − *Advanced Photonics Center, Southeast University, Nanjing 210096, Jiangsu, China*

Yizhi Zhang − *Advanced Photonics Center, Southeast University, Nanjing 210096, Jiangsu, China*

Hong Wang − *Department of Laboratory Medicine, The First Affiliated Hospital of Nanjing Medical University, Nanjing 210029, China*

Complete contact information is available at: https://pubs.acs.org/10.1021/acsomega.0c05417

Notes

The authors declare no competing financial interest.

■ ACKNOWLEDGMENTS

This work was supported by the Natural Science Foundation of Jiangsu Province (BK20201261), the Natural Science Foundation of China (NSFC) (61822503), the Zhishan Scholars Program of Southeast University, the Fundamental Research Funds for the Central Universities and the National Key Basic Research Program of China (2015CB352002).

■ REFERENCES

(1) Huang, B.; Babcock, H.; Zhuang, X. Breaking the Diffraction Barrier: Super-Resolution Imaging of Cells. *Cell* **2010**, *143*, 1047−1058.

(2) Huang, B.; Bates, M.; Zhuang, X. Super-Resolution Fluorescence Microscopy. *Annu. Rev. Biochem.* **2009**, *78*, 993−1016.

(3) Patterson, G.; Davidson, M.; Manley, S.; Lippincott-Schwartz, J. Superresolution Imaging using Single-Molecule Localization. *Annu. Rev. Phys. Chem.* **2010**, *61*, 345−367.

(4) Hein, B.; Willig, K. I.; Hell, S. W. Stimulated emission depletion (STED) nanoscopy of a fluorescent protein-labeled organelle inside a living cell. *Proc. Natl. Acad. Sci. U. S. A.* **2008**, *105*, 14271−14276.

(5) Hell, S. W.; Wichmann, J. Breaking the diffraction resolution limit by stimulated emission: stimulated-emission-depletion fluorescence microscopy. *Opt. Lett.* **1994**, *19*, 780−782.

(6) Gustafsson, M. G. L. Nonlinear structured-illumination microscopy: wide-field fluorescence imaging with theoretically unlimited resolution. *Proc. Natl. Acad. Sci. U. S. A.* **2005**, *102*, 13081−13086.

(7) Xia, T.; Li, N.; Fang, X. Single-Molecule Fluorescence Imaging in Living Cells. *Annu. Rev. Phys. Chem.* **2013**, *64*, 459−480.

(8) Betzig, E.; Patterson, G. H.; Sougrat, R.; Lindwasser, O. W.; Olenych, S.; Bonifacino, J. S.; Davidson, M. W.; Lippincott-Schwartz, J.; Hess, H. F. Imaging Intracellular Fluorescent Proteins at Nanometer Resolution. *Science* **2006**, *313*, 1642−1645.

(9) Hess, S. T.; Girirajan, T. P. K.; Mason, M. D. Ultra-High Resolution Imaging by Fluorescence Photoactivation Localization Microscopy. *Biophys. J.* **2006**, *91*, 4258−4272.

(10) Dertinger, T.; Colyer, R.; Iyer, G.; Weiss, S.; Enderlein, J. Fast, background-free, 3D super-resolution optical fluctuation imaging (SOFI). *Proc. Natl. Acad. Sci. U. S. A.* **2009**, *106*, 22287−22292.

(11) Rust, M. J.; Bates, M.; Zhuang, X. Sub-diffraction-limit imaging by stochastic optical reconstruction microscopy (STORM). *Nat. Methods* **2006**, *3*, 793−796.

(12) van de Linde, S.; Löschberger, A.; Klein, T.; Heidbreder, M.; Wolter, S.; Heilemann, M.; Sauer, M. Direct stochastic optical reconstruction microscopy with standard fluorescent probes. *Nat. Protoc.* **2011**, *6*, 991−1009.

(13) Yamanaka, M.; Smith, N. I.; Fujita, K. Introduction to super-resolution microscopy. *Microscopy* **2014**, *63*, 177−192.

(14) Biteen, J. S.; Thompson, M. A.; Tselentis, N. K.; Bowman, G. R.; Shapiro, L.; Moerner, W. E. Super-resolution imaging in live Caulobacter crescentus cells using photoswitchable EYFP. *Nat. Methods* **2008**, *5*, 947−949.

(15) Shcherbakova, D. M.; Sengupta, P.; Lippincott-Schwartz, J.; Verkhusha, V. V. Photocontrollable Fluorescent Proteins for Super-resolution Imaging. *Annu. Rev. Biophys.* **2014**, *43*, 303−329.

(16) Shimomura, O.; Johnson, F. H.; Saiga, Y. Extraction, Purification and Properties of Aequorin, a Bioluminescent Protein from the Luminous Hydromedusan, Aequorea. *Journal of Cellular and Comparative Physiology* **1962**, *59*, 223−239.

(17) Bates, M.; Huang, B.; Dempsey, G. T.; Zhuang, X. Multicolor Super-Resolution Imaging with Photo-Switchable Fluorescent Probes. *Science* **2007**, *317*, 1749.

(18) Jones, S. A.; Shim, S.-H.; He, J.; Zhuang, X. Fast, three-dimensional super-resolution imaging of live cells. *Nat. Methods* **2011**, *8*, 499−505.

(19) Hoyer, P.; Staudt, T.; Engelhardt, J.; Hell, S. W. Quantum Dot Blueing and Blinking Enables Fluorescence Nanoscopy. *Nano Lett.* **2011**, *11*, 245−250.

(20) Xu, J.; Tehrani, K. F.; Kner, P. Multicolor 3D Super-resolution Imaging by Quantum Dot Stochastic Optical Reconstruction Microscopy. *ACS Nano* **2015**, *9*, 2917−2925.
(21) Dempsey, G. T.; Vaughan, J. C.; Chen, K. H.; Bates, M.; Zhuang, X. Evaluation of fluorophores for optimal performance in localization-based super-resolution imaging. *Nat. Methods* **2011**, *8*, 1027−1036.
(22) Ha, T.; Tinnefeld, P. Photophysics of Fluorescent Probes for Single-Molecule Biophysics and Super-Resolution Imaging. *Annu. Rev. Phys. Chem.* **2012**, *63*, 595−617.
(23) Ha, T.; Enderle, T.; Ogletree, D. F.; Chemla, D. S.; Selvin, P. R.; Weiss, S. Probing the interaction between two single molecules: Fluorescence resonance energy transfer between a single donor and a single acceptor. *Proc. Natl. Acad. Sci. U. S. A.* **1996**, *93*, 6264−6268.
(24) Jares-Erijman, E. A.; Jovin, T. M. FRET imaging. *Nat Biotech* **2003**, *21*, 1387−1395.
(25) Roy, R.; Hohng, S.; Ha, T. A practical guide to single-molecule FRET. *Nat. Methods* **2008**, *5*, 507−516.
(26) Yuan, L.; Lin, W.; Zheng, K.; Zhu, S. FRET-Based Small-Molecule Fluorescent Probes: Rational Design and Bioimaging Applications. *Acc. Chem. Res.* **2013**, *46*, 1462−1473.
(27) Baker, S. N.; Baker, G. A. Luminescent Carbon Nanodots: Emergent Nanolights. *Angewandte Chemie International Edition* **2010**, *49*, 6726−6744.
(28) Markovic, Z. M.; Ristic, B. Z.; Arsikin, K. M.; Klisic, D. G.; Harhaji-Trajkovic, L. M.; Todorovic-Markovic, B. M.; Kepic, D. P.; Kravic-Stevovic, T. K.; Jovanovic, S. P.; Milenkovic, M. M.; Milivojevic, D. D.; Bumbasirevic, V. Z.; Dramicanin, M. D.; Trajkovic, V. S. Graphene quantum dots as autophagy-inducing photodynamic agents. *Biomaterials* **2012**, *33*, 7084−7092.
(29) Shen, J.; Zhu, Y.; Yang, X.; Li, C. Graphene quantum dots: emergent nanolights for bioimaging, sensors, catalysis and photovoltaic devices. *Chem. Commun.* **2012**, *48*, 3686−3699.
(30) Chen, H.; Wang, Z.; Zong, S.; Chen, P.; Zhu, D.; Wu, L.; Cui, Y. A graphene quantum dot-based FRET system for nuclear-targeted and real-time monitoring of drug delivery. *Nanoscale* **2015**, *7*, 15477−15486.
(31) Hummers, W. S., Jr.; Offeman, R. E. Preparation of graphitic oxide. *J. Am. Chem. Soc.* **1958**, *80*, 1339−1339.
(32) Crosby, G. A.; Demas, J. N. Measurement of photoluminescence quantum yields. Review. *J. Phys. Chem.* **1971**, *75*, 991−1024.
(33) Chan, W. C.; Nie, S. Quantum Dot Bioconjugates for Ultrasensitive Nonisotopic Detection. *Science* **1998**, *281*, 2016.
(34) Biju, V.; Itoh, T.; Anas, A.; Sujith, A.; Ishikawa, M. Semiconductor quantum dots and metal nanoparticles: syntheses, optical properties, and biological applications. *Anal. Bioanal. Chem.* **2008**, *391*, 2469−2495.
(35) Yang, K.; Wan, J.; Zhang, S.; Tian, B.; Zhang, Y.; Liu, Z. The influence of surface chemistry and size of nanoscale graphene oxide on photothermal therapy of cancer using ultra-low laser power. *Biomaterials* **2012**, *33*, 2206−2214.
(36) Magde, D.; Rojas, G. E.; Seybold, P. G. Solvent Dependence of the Fluorescence Lifetimes of Xanthene Dyes. *Photochem. Photobiol.* **1999**, *70*, 737−744.

https://doi.org/10.1021/acsomega.0c05417
ACS Omega 2021, 6, 8808−8815